Localised surface vibration and acoustic noise emitted from laboratory scale transformer cores assembled from grain-oriented electrical steel

Anthony J Moses[1], *Member, IEEE,* Philip I. Anderson[1] and Teeraphon Phophongviwat[2]

[1]Wolfson Centre for Magnetics, Cardiff School of Engineering, Cardiff University, Cardiff, CF24 3AA, United Kingdom
[2]Dept. of Electrical Engineering, King Mongkut's Institute of Technology, Ladkrabang, Bangkok, 10520, Thailand

Magnetostriction of grain-oriented 3% Si Fe sheets was measured prior to assembly into model transformer cores. Core vibration was measured using a laser scanning vibrometer and harmonic spectra of acoustic noise were evaluated from the microphone outputs. Explanations show why no correlation exists between vibration harmonics profiles and A-weighted acoustic noise spectra. High localised vibration did not cause high noise due to phase differences in surface vibrations and it is shown that this is the main reason why the A-weighted noise of a three phase core can be less than that of an equivalent single phase core. Noise from cores assembled from low magnetostriction materials was not always lowest because of the variable effect of electromagnetic forces.

***Index Terms*—Acoustic noise, electrical machine cores, electrical steels, magnetostriction, transformer cores, vibration.**

NOMENCLATURE

A_c	Limb cross sectional area
A_{cn}	Cross sectional areas of clamping bolt
B_c	Critical flux density
B_g	Gap Flux densityB_p Peak flux density
B_n	Interlaminar flux density
B_p	Peak flux density
B_s	Saturation magnetisation
CGO	Conventional grain-oriented silicon steel
EM	Electromagnetic
GO	Grain-oriented silicon steel
HGO	High permeability grain-oriented silicon steel
Hz	Hertz
J	Bolt torque coefficient
K	Environmental correction factor
LDR	Domain refined HGO
L_{pA}	Corrected average A-weighted sound pressure level
L_{pA0}	Average A-weighed sound pressure level
L_{pi}	Sound pressure level
L_{pAi}	A-weighed sound pressure level for each microphone
L_{bgA}	Average A-weighted background noise pressure level
MS	Magnetostriction
MSL	Multi-step lap
N	Number of steps in a MSL joint
N_{mic}	Number of microphones in the array
N_s	Number of secondary turns
RD	Rolling direction of electrical steel sheet
SSL	Single-step lap
T	Bolt clamping torque
V_{av}	Average value of induced voltage
b	Instantaneous flux density
e	Flux eccentricity ratio
d_b	Bolt diameter
f	Magnetising frequency
h	Height of segment
l	Length of lamination
p_i	Sound pressure
p_{ref}	Reference pressure
r	Circle radius
rms	Root mean square
s_{pp}	Peak to peak displacement
ε	Strain
σ_n	Surface clamping stress
ω	Angular frequency ($\omega = 2\pi f$)
v_{rms}	Root mean square of surface velocity
θ	Subtended angle
δl_λ	Magnetostrictive strain
δl_t	Total strain
δl_M	Strain due to electromagnetic force
$\mu\varepsilon$	Micro-strain

Manuscript received January 30, 2016 (date on which paper was submitted for review). Corresponding author: A.J Moses (e-mail: Mosesaj@cf.ac.uk).
Digital Object Identifier inserted by IEEE

I. INTRODUCTION

The origins of acoustic noise emitted by a power transformer core and ways of controlling it have been studied for many decades. Today the demand for low noise transformers is growing rapidly as more units are being sited in urban areas where size and weight rule out some established methods of noise limitation. The magnetic core vibration during the magnetising process is the primary source of the noise but the noise emitted from the fully assembled transformer is determined by its transmission through the cooling oil, etc. to the tank and how the tank then radiates the sound. The core vibration depends on many factors including the magnetostrictive properties of the magnetic core material, the design of corner joints in the stacked core, accurate positioning of lamination within the core and also careful mechanical design of all components in the transformer to minimise resonance effects.

It is generally accepted that the two dominant sources of core noise are vibrations due to MS and EM forces but to date no method of estimating the contribution each makes to the noise of a given transformer core has been established. Contribution to knowledge and understanding of the mechanisms given in this paper will help in formulating suitable prediction methods.

Power transformer cores, and most distribution transformer cores, are assembled from laminations of electrical steel, grain-oriented 3% SiFe (GO). Commercial grades of GO can be grouped into three categories: conventional grain-oriented material (CGO), high permeability material (HGO) and domain refined HGO (LDR). MS of GO is very sensitive to mechanical stress which might be present in cores as a result of design or assembly [1]. However, no definite relationship between MS and core noise to quantify the benefit of using low MS material has been established.

EM forces occur in laminated cores mainly where magnetic flux transfers between layers of laminations in core joints or jumps across air gaps between laminations at the joints. The small localised movement caused by these forces is a source of core vibration and noise. Today multi-step lap (MSL) joints [2] are widely used in stacked cores of distribution transformer primarily to reduce core losses but a further benefit is that the corner joint flux distribution is more favourable hence causing localised EM forces to be lower than those occurring in a single-step lap (SSL) joint which in turn results in quieter cores.

It is difficult to determine what proportions of localised vibration of a core surface are due to MS or EM forces since at any position, one may dominate or they can be of the same order of magnitude. If the core flux density varies sinusoidally at 50 Hz, the vibration waveform will comprise a fundamental component at 100 Hz with a series of superimposed harmonics. Although these harmonics are mainly much lower in magnitude than the fundamental component, the noise they produce can be a major source of annoyance because of the frequency sensitivity of the human ear, e.g., the ear is around 10 times more sensitive to a 1000 Hz component of noise than one at 100 Hz.

Some important previous findings relevant to the investigation are given below together with some representative references:

(a) Use of GO with low stress sensitivity of MS gives low core noise [1]-[5]
(b) Vibration due to localised MS and EM forces are the source of core noise [6]-[11]
(c) Noise from MSL cores is generally lower than that of SSL assemblies [3]- [5], [6], [10]-[14]
(d) Core clamping methods have a major effect on noise [4], [8], [9], [12], [15]
(e) MS velocity is a more relevant parameter to use than displacement when attempting to quantify the effect of MS on transformer noise [2], [4], [5], [13], [16]
(f) The harmonics of MS and core vibration are at least as influential on core noise as the fundamental component [4], [6], [13], [17]- [19]
(g) In three limb cores, the surface vibration is highest in the T-joints and the outer corners [5], [8], [20]

However, these findings are not quantified and sometimes concluded from a limited number of tests or observations. An important fact not widely appreciated in previous studies is that the out of plane surface vibration of the middle limb of a three phase, three limb core is 180° out of phase with that of the outer two limbs. This of course means that it is unlikely that a close correlation will exist between averaged peak vibration measurements, as commonly presented previously, and acoustic noise. In an investigation of load noise reported in [20] it is pointed out that this sort of phase difference results in a directed noise radiation. Earlier it was shown that the fundamental (1st harmonic) out of plane vibration of the centre limb of a three phase core was 180° out of phase with the vibration of the outer limbs but its relevance to transformer noise was not discussed [21].

This paper reports on findings of a systematic study of noise and vibration of model transformer cores aimed at increasing our knowledge of the phenomena as well as expanding on some of the above findings. The emphasis of the work was to further our understanding of the fundamental mechanisms of core vibration and their influence on the noise. The use of smaller model cores enabled key parameters to be investigated whilst limiting the variation of other factors in the cores design, manufacture and operation. In the investigation, MS characteristics of single sheets of GO were measured before laminations were cut from the same batches of steel and assembled as transformer cores. The surface vibration distribution and acoustic noise outputs of the cores were systematically measured and analysed.

II. Experimental procedures

A. Magnetostriction measurement

The peak to peak magnitude of the MS strain of GO, measured along its rolling direction (RD), is less than 1 $\mu\varepsilon$ (micro-strain) and only varies a small amount between best and standard grades of steel in a stress free state. However, when compressive stress is applied along the RD, MS increases rapidly to over 20 $\mu\varepsilon$ in a manner dependent on the steel's texture and surface coating. It is generally found that use of grades of GO with low sensitivity to core building stresses lead to low noise cores [2], [3].

An established MS measurement system [22] was used as a model for an upgraded dedicated system [23] used in this investigation in which longitudinal stress of up to ±10 MPa could be applied during measurements to quantify the stress sensitivity of MS of strips of grades of steels chosen to assemble the studied cores. The peak to peak MS and mean vibration velocity of single strips of GO were measured at 50 Hz sinusoidal flux density. Commercial grades of 0.30 mm thick CGO, HGO and LDR were selected. Fig. 1 shows representative MS characteristics measured along their RDs magnetised along the same direction at low and high flux density. The uncertainty in the measurement of peak to peak MS was around ± 3.5 % of the recorded values.

FIG. 1 HERE

The main points to note from the characteristics in Fig. 1 are:

(a) Under tension or zero stress the magnitude of the MS of each material is less than ± 0.6 $\mu\varepsilon$ at both flux densities implying that the MS induced noise might be very low in a stress free core and similar for each material.
(b) As flux density is increased from 1.0 T to 1.7 T, the critical compressive stress, at which MS begins to rise rapidly, falls by 30 % (CGO), 60 % (LDR) and 20 % (HGO) from

initial values of around -1.5, -4.0 and -5.0 MPa. This implies that the MS induced noise in a moderately stressed LDR core will increase more with increasing flux density than in a similarly stressed HGO core.

In terms of MS improvement, the stress range over which HGO is advantageous over LDR is around -4.0 MPa to -7.5 MPa at low flux density and between -2.0 MPa and -7.5 MPa at high flux density. This demonstrates the possible desirability of quantifying and, if feasible, controlling the building stress in cores to optimise material selection. However, the potential noise reduction benefit of HGO over CGO is significant over the full compressive stress range.

It should be noted that the materials were selected to provide a wide range of magnetostrictive behavior and not to be representative of the individual grades, so no wider conclusions should be drawn from these initial results.

These observations of course only refer to MS induced noise and, even then, rotational MS in the T-joints, which locally can be much larger than that occurring along the RD [24], and the harmonic content of the MS characteristic are not considered here.

B. Core magnetization and measurement system

Fig. 2 shows an overview of the transformer core testing system. A three phase core was magnetised by a 15 kVA, three phase autotransformer whose output voltages were adjusted to produce balanced flux density in the three-phase, three-limb core under test (one phase of the autotransformer was used for energising single phase cores). The power analyser was used to monitor induced voltages in 30 turn secondary windings wound around each limb. Prior to each noise or vibration measurement, the voltage induced in each coil was adjusted to produce peak flux density B_p given by

$$B_p = {}^{V_{av}}/_{4.44 f N_s A_c} \quad \text{T} \tag{1}$$

where V_{av} is the average value of the induced voltage, f is the magnetising frequency, N_s is the number of secondary winding turns and A_c is the cross sectional area of the core limb. The limb flux densities were maintained sinusoidal to within a form factor tolerance of 1.11±0.2 %.

The transformer under test was placed vertically in a 2.0 m by 3.5 m by 2.2 m (height) hemi-anechoic acoustic chamber whose surfaces were covered with highly absorbent materials to avoid acoustic reflections.

FIG. 2 HERE

A laser scanning vibrometer was used to measure the vibration profile of selected areas of the core surface. An array of microphones with matching amplifiers was used to obtain the sound pressure distribution at a fixed distance from the core surface. The measurement data was analysed using LabVIEW and Matlab. Fig. 3 shows a transformer under test with the vibrometer positioned above the core. The detailed methodologies are described in the following sub sections.

FIG. 3 HERE

C. Vibration measurement methodology

A Polytec PSV-400 scanning vibrometer was used to measure the localised core vibration. Associated software provided graphics and animation in the form of 2-D colour maps. The system was capable of measuring instantaneous surface velocity in the range 0.01μm/s to 10m/s. Instantaneous and rms components of vibration velocity perpendicular to the plane of the laminations and the corresponding frequency spectra were averaged over 10 mm × 10 mm surface areas. The manufacturer's quoted maximum measurement error was less than ±1.3 %.

Mirrors, such as the one shown on the right hand side of the core in Fig. 3, were used to scan three surfaces of the core under test without needing to move the vibrometer. A Polytec PSV 8.8 Single point vibrometer was used to compensate the output of the PSV-400 Scanner for any spurious room vibrations. The average of three velocity reading was calculated at each measurement point during core testing.

D. Acoustic noise measurement

Conditions for measuring noise of commercial transformers as specified in IEC 60076-10 2001 "Power transformers-Part 10: Determination of sound levels" were followed in this investigation. An array of eight B&K 4188-A-021 condenser microphones with frequency response range of 8 Hz to 12.5 kHz was positioned at half the height of the core with each microphone located 300 mm from the core surface as shown in Fig. 4. A virtual instrument (VI) was developed to determine the sound pressure and the sound pressure level detected by each microphone as well as the averaged A-weighted sound pressure and level (corrected for background noise). The sound detected by each microphone was measured simultaneously.

FIG. 4 HERE

The measured sound pressure levels are independent of the environment and the distance of the microphones from the core so the sound pressure and the sound pressure level recorded by each microphone could be analysed in A-weighted true acoustic terms [25]. To do this, initially, the sound pressure p_i was calculated at each microphone position from its output voltage and sensitivity. The sound pressure level L_{pi} was calculated from

$$L_{pi} = 20 \times log_{10}\left(\frac{p_i}{p_{ref}}\right) \quad \text{dB} \tag{2}$$

where the reference pressure p_{ref} is taken to be 20×10^{-6} Pa which is approximately the threshold of human hearing at 1000 Hz. The A-weighted sound pressure level L_{pA0} averaged for all the microphones is given by

$$L_{pA0} = 10 \times log_{10}\left(\frac{1}{N_{mic}} \sum_{i=1}^{N_{mic}} 10^{\frac{L_{pAi}}{10}}\right) \quad \text{dBA} \tag{3}$$

where L_{pAi} is the A-weighed sound pressure level for each microphone and N_{mic} = 9 (the number of microphones). This equation was modified as below to incorporate the average A-weighted background noise pressure L_{bgA} and an environmental correction factor K which also corrected for the different radiating surfaces so noise output from three phase and single phase cores could be compared unambiguously [25].

$$L_{pA} = 10 \times log_{10}\left(10^{\frac{L_{pA0}}{10}} - 10^{\frac{l_{bgA}}{10}}\right) - K \quad \text{dBA} \qquad (4)$$

The correction for background noise was applied after each live noise measurement. Its average value was only 22 dBA so any error it might cause would be insignificant.

E. Core design and test procedure

Cores were assembled from 100 mm wide laminations. Fig. 5 shows the overall dimensions and assembly of single and three phase cores. Approximately 250 layers of laminations were used. The total core masses of the three phase and single phase assemblies were 115 kg and 72 kg respectively. Resonant vibrations modes of this core geometry were calculated to confirm that they would not influence the investigation.

FIG. 5 HERE

The cross-hatched areas are the regions over which localised vibrations were measured. Examples of the SSL and MSL joints used are shown in Fig. 6. The MSL assembly comprised four steps with an overlap length of 0.3 mm using one lamination per layer. Three laminations per layer were used in the SSL step cores with a 6 mm overlap. Fig. 6 shows the assembly of typical SSL and MSL corner joints.

FIG. 6 HERE

Previous reports on the dependence of core noise on the number of laminations per step layer and the overlap length present conflicting conclusions. For example [3] and [14] conclude that 3 to 4 step laps is the optimum number whereas [12]-[15] state that 3 steps should be avoided. Also [3] and [14] report that using 2 or 3 laminations per layer instead of one has a marginal effect on noise whereas [13] and [26] say that this increases noise. Early comprehensive work on single phase cores showed that the noise increases monotonically with increasing overlap length in SSL joints [27] whereas [12] and [14] state overlap length of 2 mm should be avoided. The apparently conflicting results in these examples are most likely due to the fact that the many variables associated with core design, material selection, magnetisation level, etc., which influence the variation of noise with joint design, are not likely to be the same in each investigation so differing conclusions are not surprising. Hence the corner joint configurations chosen for this investigation were based on practicality and experience taking into account the previous findings.

As mentioned in section I, the core clamping method has a large influence on noise. In this investigation 50 mm by 30 mm wooden clamping plates were positioned on either side of each yoke and 30 mm × 20 mm plates on each limb as shown in Fig. 5. The clamping plates are secured by 8 mm diameter reinforced plastic bolts (14 in all for the three phase core) each tightened to a torque of 4.0 Nm for the main tests. The average out of plane component of surface clamping stress σ_n depends on the position and number of core clamps, in this configurations it is calculated from [28]

$$\sigma_n = T/Jd_b\,A_{cn} \qquad \text{Pa} \qquad (5)$$

where T is the bolt torque, J is the torque coefficient (assumed as 0.45 for such steel bolts), d_b is the bolt diameter and A_{cn} is the cross sectional area to which the bolt force is applied. The stress on each layer of laminations varies with depth into the core and drops moving away from each bolt. In this case $\sigma_n \approx 0.08\ T$. Hence, if each bolt is tightened to 4.0 Nm, the average normal stress at the core surface is 0.33 MPa.

F. Measurement of localised flux density in a core

Because of GO's large grains and high in-plane anisotropy and the complex three dimensional flux paths, it has so far been impossible to accurately predict localised components of flux density in the joints using computational electromagnetic solvers so time consuming experimental methods are still necessary. Laminations from one layer of a core were selected for hosting search coils for localised flux density measurements. An array of 10 mm long, single turn 0.19 mm diameter enamel covered copper wire search coils was wound through 0.5 mm diameter holes drilled in the laminations.

The laminations were assembled in the central region of a three phase, MSL CGO core which was magnetised as described in section III *A*. The magnitude and phase of the emf's induced in the pairs of orthogonal coils were measured and the instantaneous magnitude and direction of the localised flux at each point was calculated using a well-established technique [29].

III. Preliminary Measurements

A. Reproducibility of measurements

Since only small changes in core characteristics might occur due to controlled changes in joint geometry, clamping stress, core material, etc., the reproducibility and random building variability of the noise measurements was first determined. The noise output of a single phase MSL was measured using the procedure outlined in section II and the measurement repeated three times after re-magnetising to nominal flux densities of 1.5 T to 1.8 T. The core was next dismantled and reassembled and the sequence of measurements repeated. The repeatability of measurements on the assembled core was within ± 0.5 dBA whereas the variation after re-assembly increased from around 1.0 dBA at 1.5 T to 4.0 dBA at 1.7 T and 1.8 T. Build variations of ±6 dBA, and even higher for individual harmonics, have been reported for MSL cores [14], [15] so the careful building practice adopted here made the variations as low as practically achievable.

To determine the variation in noise of identical transformers assembled from laminations from the same batches of materials, pairs of SSL and MSL three phase cores were assembled and tested. Four cores of each material, two with SSL joints and the other two with MSL joints, were magnetised between 1.5 T and 1.8 T with bolt torques of 4.0 Nm.

A small difference of 1.5 dBA on average, between the noise of nominally identical transformers in the other pairs can be attributed to core build variations. The noise of the MSL cores was on average 4 dBA lower than that of equivalent SSL cores. The noise of the CGO cores was consistently higher than cores assembled from the other materials presumably due to their poorer stress sensitivity.

B. Variation due to clamping

In order to assess the effect of the clamping method, a three phase, MSL core assembled from CGO was clamped tightly for confirming the limbs were flexing rigidly at bolt torques of 2.0 Nm to 6.0 Nm. The A-weighted sound pressure level emitted from the core was measured at three microphone locations. It was found that the noise did not vary with clamping pressure any more than could be attributed to normal build variations. Previous reports show that noise increases by around 3 dBA as clamping torque increases from 15 Nm to 30 Nm [26] but [4] reported an optimum clamping stress in the range 0.075 MPa to 0.10 MPa according to joint design and operating flux density. Unsurprisingly, this is not much less than the 0.33 MPa (4.0 Nm bolt torque) value found here, which itself is a maximum localised value obtained from (5), so is far lower than the average value throughout the core.

The dependence of surface vibration on clamping stress was investigated using the laser scanning vibrometer. Fig. 7 shows the surface vibration patterns observed on the front surface of a CGO core magnetised at 1.7 T under different clamping torques. The figure shows the localised, out of plane rms component of velocity over the surface area depicted by the hatched areas in Fig. 5, i.e. over lamination surfaces in the upper right hand portion of the core including regions in the T-joint and corner joint not obstructed by the clamps. The anticipated highest vibration velocity occurs in regions of the T-joint and centre limb as well as the outside corner joint at all three clamping pressures. There is high lamination flapping in the outer joint at 2.0 Nm and a significant increase in vibration in the centre limb at the high clamping stress.

The vibration amplitude appears to increase with increasing clamping stress although the acoustic noise dropped at an intermediate clamping stress. It is shown in sections IV that a direct correlation between rms surface velocity and noise output should not be expected.

Since a clamping torque of 4.0 Nm has least effect on noise it was decided to use this setting throughout the investigation.

FIG. 7 HERE

In order to fully understand the vibrometer measurements it is useful to develop the basic relationship between rms velocity of a surface and the corresponding displacement. Suppose a lamination is vibrating sinusoidally in time at frequency ω, the driving force being magnetostrictive or electromagnetic. If one end of the lamination is fixed and it is vibrating in its plane then the peak to peak displacement of the other end during each cycle of magnetisation is given simply by

$$s_{pp} = \sqrt{2}\, v_{rms}/\omega \quad \text{metre} \tag{6}$$

where v_{rms} is the rms velocity. If we take an example of a typical measured velocity of 1. 0 mm/ s and frequency of 100 Hz, typical of the measurements being presented in this work, then s_{pp} = 2.2 μm. If this occurs on a 550 mm long yoke lamination then the peak to peak strain is 2 $\mu\varepsilon$. In practice the velocity will change sinusoidally in time but this example shows that the magnitude of the associated displacement is compatible to that of MS in GO.

C. Noise distribution pattern around a core

Noise output of each core was normally calculated as described in section II *D* by averaging the outputs of the microphones at locations shown in Fig. 4 using the IEC guidelines. However initially it was decided to measure the variation of noise around a core from the outputs of the individual microphones. A CGO three phase MSL core was placed in the chamber and magnetised at 1.0 T to 1.8 T. The A-weighted noise output from each microphone was recorded separately to produce the distribution shown in Fig. 8. At high flux density the noise detected by the microphones opposite the two sides of the central limb is 4-5 dBA higher than that measured at any other position but at 1.0 T it was only marginally higher. The noise detected above the core (position 9) was generally lower than that detected by microphones positioned around the core. The higher than average noise level adjacent to the centre limb is possibly due to larger vibration in that limb as will be seen later.

Examining the noise detected by the individual microphones in this way can help identify regions where high vibration occurs. Unless stated otherwise, the noise measurements presented in the later sections are all the average of the nine microphone readings which was found to reduce the measurement uncertainty, due primarily to the relative positioning of the microphones and core, to less than ±2 %.

FIG. 8 HERE

IV. Experimental Measurements and Analysis

A. Core front surface noise and localised vibration

The harmonic spectrum of the vibration at the selected points on the core surface shown in Fig. 9 was investigated. At points A, B and C the core was expected to be subjected mainly to alternating flux density along the RD of the laminations. At D, within the T-joint region, rotational magnetisation occurs and out of RD components of flux [35] could occur at E, in the

corner region. Any differences in vibration measured at A, B, C could be attributable to non-uniform clamping stress with position C being furthest from the most highly stressed region under the clamp or localised flux distortion but no differences were actually found

FIG. 9 HERE

Table I shows the results when magnetised at 1.0 T to 1.7 T. No significant difference between the vibration characteristics at A/B/C was apparent so the values are averaged in the table. It is noticeable that the vibration at the locations outside the corners is dominated by the fundamental (100 Hz). At points D and E the higher harmonics are significant, undoubtedly related to complex localised magnetisation or rotational MS [24] in the joint regions.

Localised flux density measurements were made to help estimate the importance of rotational MS in this case. The laminations on which localised search coils were mounted as described in section II *F* were inserted into the centre region of the core. The localised flux density was measured while the core was magnetised sinusoidally at 1.7 T. In central regions of the yokes and the limbs the localised flux contained up to 9.4 % 3rd harmonic components distributed in a random manner as expected [30]. At the outer corner joints, the harmonic content increased to 38.1 % but the transverse component of flux did not exceed 0.13 T when the peak flux density in the RD was 1.7 T.

An important finding supporting early work [31] is that at no point in the T-joint did the flux eccentricity ratio (e = peak value of TD component / peak value of RD component) exceed 0.2. This was not surprising since it has been claimed that rotational flux in a T-joint is highly elliptical and "pure rotational flux (e= 1.0) does not normally occur in such transformer cores [32]. This has important implications on the widely promoted view that rotational magnetostriction (i.e. due to pure rotational flux) is a major cause of core vibration [10].

TABLE 1 HERE

The frequency spectrum of the sound pressure at the front surface of the same CGO MSL core was measured and the results are summarised in Fig. 10. The 100 Hz (fundamental) component only dominates at low flux density whereas the second and third harmonics become prominent at the higher flux densities.

FIG. 10 HERE

The average sound pressure (Pa) from a measurement system in the time domain is converted to sound pressure level (dB) in the frequency domain using (2) and then transformed to the A-weighted sound pressure level (dBA). It can be noted that although the sound pressure (and proportional sound pressure level) is lower at 1.5 T than at 1.0 T, the corresponding A-weighted value is higher at 1.5 T. This demonstrates the impact of allowing for the response of the human ear by A-weighting. However, there is no correlation between the distribution of vibration and noise harmonics in Tables III associated with different regions of the core.

The equivalent components of out of plane rms vibration patterns on the front surface of the core magnetised at 1.0 T to 1.7 T are shown in Fig. 11. No correlation with the noise measurement data presented in Fig.10 is apparent but the average corner and central limb vibration is two to over four times higher than that in the yoke, the factor increasing with increasing flux density confirming that these regions are the source of highest vibration in three phase cores. The rms velocities averaged over the corner regions, the centre limb and T-joints are shown on the contour distributions to help quantify the effect.

FIG. 11 HERE

Although A-weighted sound power level is gaining acceptance as a reference quantity for quantification and comparison of noise generated from transformer cores, it is not suitable for investigating the relationship between noise and vibration because the A-weighting scale is applied to the sound pressure signal. Sound pressure and the vibration signal in the frequency domain are the most appropriate parameters for studying the relationship between transformer core noise and vibration.

B. Core side and top surface noise and localised vibration

Core noise and vibration was measured with respect to side and top surfaces of the CGO MSL core using the same approach as presented in the previous section. Fig. 12 show the harmonic spectrum of the velocity recorded at the positions indicated in Fig. 10 on the top (points F, G and H) and side (points I and J) surfaces of the core. At 1.0 T very little harmonic distortion was observed. Even at the higher flux densities the fundamental component and harmonics are far lower than found on the front surface. The results show that the rms velocity components on the side surface are even lower than on the top surface. Only a small number of measurement points are considered here but they are representative of the low harmonic components in the vibration of the side and top surface.

FIG. 12 HERE

Table II shows corresponding frequency spectra of the sound pressure associated with the side and top surface of the core from microphones 1 and 9 respectively. Obviously they are not directly related to the localised rms velocity data just presented since the microphones are sensitive to envelopes of sound emitted from large regions of the core whereas the vibration measurements are spot readings.

TABLE 2 HERE

The sound pressure associated with the side surface is higher than that of the top surface although significantly less than the front surface. The harmonic components of both increase with

flux density possibly due to the increasing prominence of MS harmonics [32] although generally they are lower than the equivalent noise harmonics shown in Table IV associated with the front surface of the core.

The 100 Hz components measured at the side and edge of the core was consistently around 65 % and 83 % respectively lower than on the front surface over the full flux density range but there is not obvious trend with the higher harmonics. The 200 Hz and 300 Hz harmonic components measured adjacent to all three surfaces dominate at 1.5 T and 1.7 T but the varying harmonic distributions are not reflected in the noise characteristics detected by the individual microphones as shown in Fig. 9**.**

The vibration pattern over the top and side core surfaces are presented in Fig. 13 and Fig. 14 respectively. It can be seen from Fig. 13 that the highest vibration velocity at any point on the top surface is around 50 μm/s and 300 μm/s at 1.0 T and 1.7 T respectively compared with equivalent values of 200 μm/s and 1000 μm/s on the front face of the core as shown in Fig. 11.

FIG. 13 HERE

FIG. 14 HERE

Also the vibration velocity of the top surface above the centre limb and outer limb is two to three times higher than in the centre of the yoke region. This can be attributed to the extension of the limbs tending to bend the yoke in the normal direction (out of plane) to a small extent, whether the mechanism is simply an opening and closing of the joints or actual physical bending of the yoke laminations in their stiff transverse direction is debatable.

In an ideal case where no out of plane vibration occurs, the measured yoke top surface velocity above the limbs should be the same as the in-plane vibration of the limb laminations themselves. At 1.7 T the top surface vibration velocity is around 130 μm/s above the central limb inferring a longitudinal strain of 3 $\mu\varepsilon$ in the centre limb which could be caused by a combination of electromagnetic induced strain originating in the T-joints and a magnetostrictive strain if the laminations were stressed to around 1-2 MPa in the case of the CGO material.

The surface vibration velocity distribution over the upper 170 μm/s length of a side limb is shown in Fig. 14, (the horizontal strip where no data is shown is obscured by an external tie bolt). The average rms vibration velocity over the measured area on the side of the core at 1.0 and 1.7 T is 38 μm/s and 100 μm/s compared to 40 μm/s and 130 μm/s on the top surface and 150 μm/s and 600 μm/s on the front surface. These are arbitrary measurement areas but the results do help visualise the vibration pattern over the full core. The maximum rms vibration velocity at both flux densities is similar in magnitude to the maximum on the top surface. The non-symmetry of the distributions on the top and side faces might be due to the inherent geometrical non-symmetry of the step lap T-joint. The sound parameters measured at the microphone positions adjacent to front, top and side surface are summarised in Table III. The highest sound pressure (mPa) and corresponding pressure level (dB) is from the side surface where the surface vibration velocity is relatively low, certainly compared to the front face. Although the surface velocity of regions of the front face is very high, the sound pressure and the A-weighted noise are low. The amplitude of average rms vibration velocity of the top surface is higher than that of the side surface but the sound pressure is lower as shown in Table III. This is the effect of time phase difference between vibrations at different parts of the top surface highlighted in the next section. It should be emphasised that the values in Table III are only included to help clarify the complex relationships between localised vibration and sound profiles and they do not represent global conditions over complete core surfaces. Hence the average values have no physical meaning but help show overall trends.

TABLE 3 HERE

C. Variation of time phase of surface vibration in the three phase core

The results presented in section III B show that the front surface of the CGO core exhibited the highest out of plane vibration velocity and the 100 Hz component dominates whereas the associated acoustic noise was unexpectedly low. Fig. 11, Fig.13 and Fig.14 show the *rms velocity* distribution on the core surface which is directly related to the localised displacement but does not show information about the variation from point to point in time phase during the magnetising cycle. In this section, the effect of the 120° phase difference between the flux densities in the three limbs of the three phase core on the magnetostrictive strain and the variation of the *instantaneous* value of the 100 Hz component of out of plane velocity throughout a magnetising cycle is considered.

Figure 15 shows the theoretical variation of instantaneous magnetic flux density at four instants in a magnetising cycle assuming the fluxes in each phase vary sinusoidally and are 120° out of phase with each other. Making use of the symmetry only half of the core is shown. The reference time $\omega t = 0°$ is defined as the instant in the magnetising cycle when the flux density in the centre limb B is zero. The light grey vectors indicate the positive reference direction and the magnitude of the peak flux density. The bolder vectors represent, to the same scale, the instantaneous magnitudes and directions of b, the instantaneous flux density.

FIG. 15 HERE

The figure also gives an indication of the longitudinal magnetostrictive distortion in the laminations obtained using a Matlab model developed to visualise the deformation assuming ideal uniform flux distribution shown. It does not take rotational

magnetisation, ac magnetisation out of RD or EM forces into account.

At ωt=0°, the flux density in limb B is zero while it is 0.866 B_p in limb A and 0.866 B_p in the opposite direction in limb C where B_p is the peak value of the nominal flux density (the direction of the flux does not affect the amplitude of MS). At this instant in time the dimension of the limb B is unchanged because its flux density is zero but the yoke is deformed as it carries the circulating flux. If we assume the MS is approximately proportional to b^2 [32], then the strain in each outer limb and the yokes at this instant is 0.866^2 or 75 % of the maximum MS. This creates the possibility of equally high magnetostrictive strain in the four outer corners together with lower strain at the T-joints.

Using a similar approach, it can be deduced that at ωt=30° the strain profile shows high values at diagonally opposite corners tending to bend the core and in the T-joint region at the same time tending to push the yokes apart. It can be seen that at ωt= 60° there is no strain in limb A so the core is non-symmetrically strained and when ωt=90° all corners are again symmetrically strained.

The deformation patterns indicated in the figure are greatly exaggerated to illustrate the effect. In practice the maximum longitudinal magnetostrictive strain in mechanically stressed GO is of the order of 20 $\mu\varepsilon$ which equates to extension of around 10 μm in the core laminations here which in turn is sufficient to cause joint noise or lamination bending. This superficial overview of in-plane magnetostrictive strain variation during a cycle includes several approximations and assumptions which make any quantified values of the resulting surface velocity or displacement very uncertain but it is helpful in trying to interpret the complex variation of instantaneous out of plane vibration measurements presented in Fig. 16. It is possible that core distortion caused by this phenomenon could interact with similar distortion predicted due to core resonance e.g. [17], [33].

It is most likely that the relationship between the out of plane vibration of a core and the in plane magnetostriction is dependent on the mechnaical stiffness and rigiditiy of the corner joints which itself can vary according to the consisenecy of assembly from core to core. Further study is necessary to verify that this is the main cause and to quantify it.

FIG. 16 HERE

Fig. 16 shows the measured instantaneous out of plane surface velocity of the MSL CGO core, magnetised at 1.7 T, at the same instances in time as shown diagrammatically in Fig. 15. The surfaces where no velocity distribution pattern is shown are obscured by magnetising coils or clamps.

At ωt=0° the flux density in the middle limb is zero, the MS of the laminations in the middle limb is also zero but the limbs are possibly subjected to forces at their ends due to the MS in the yoke laminations which is a possible explanation of the low small vibration in the middle limb shown in Fig. 15 at ωt=0° or ωt=180°. However, at the same instant in time the highest vibration is close to one pair of diagonally opposite corners which cannot be explained from the magnetostrictive strain postulated in Fig. 15.

The model in Fig. 15 only shows the relationship between magnetizing signal and MS but Fig. 16 shows the effect of both MS and magnetic forces on the core. Because vibration displacement is not only magnetostrictive, zero core vibration velocity occurs when core vibration displacement is zero but not necessarily when MS is zero.

At ωt=30° the velocity of the central limb is highest although the MS of limb C is highest at this time. At ωt=90° the vibration of the middle limb has risen to its maximum amplitude. Although no experimental observations could be made at the centre of the middle limb, it can be assumed from the trend that the highest vibration of the middle limb is at its centre with amplitude approximately twice that of the outer limbs. This is seen in Fig. 17 which compares the time phase of the bending motion of the three limbs. It will be noted from Fig. 11 that at 1.5 T the average rms velocity in the centre limb is around 0.55 mm/s and in limb C it is around 0.30 mm/s implying peak values of around 0.80 mm/s and 0.40 mm/s respectively whereas the respective peak values in Fig. 17 are 2.0 mm/s and 1.0 mm/s respectively. This difference is because the rms value of the total vibration is considered in Fig. 11 whereas the peak value of the 100 Hz component is presented in Fig. 16. This clearly shows that the vibration velocity of the outer two limbs is around 180° out of phase with that of the centre limb. Hence the acoustic waves generated at the surface of the centre limb, which is vibrating at double the amplitude of the outer limbs, will be cancelled out to a large extent by those generated by the motion of the outer two limbs, the amount of cancellation being proportional to the cosine of the phase difference between the waves [25] which in this case (cos 180°) results in optimum cancellation in the three limbs at 1.5 T.

FIG. 17 HERE

D. Comparison of surface vibration modes and harmonics in SSL and MSL cores.

Surface vibration studies were made on CGO three phase SSL and MSL cores in order to see if any correlation with the noise outputs was apparent. Fig. 18 shows the rms velocity patterns on the front surface of the SSL and MSL CGO cores at 1.0 T and 1.7 T. (Figures 18(b) and 18(d) are duplicates of Figures 11(a) and 11(c) and are added for clarity). Interestingly the vibration of the centre limb is higher than that of the outer limb and yoke but it is higher at both flux densities in the MSL configured core although its noise output was lower as shown earlier. The average value of the rms velocity over the whole measured surface area at 1.0 T for the SSL and the MSL cores were 0.14 mm/s and 0.20 mm/s and the corresponding values at 1.7 T were 0.57 mm/s and 0.74 mm/s respectively.

FIG. 18 HERE

An interesting phenomenon, not clearly visible in Fig.18. is the high vibration due to asymmetrical structure of the SSL design at 1.7 T. The same effect is present at 1.5 T.

The rms in-plane velocity distribution was also measured on the top and side surface of the two cores. The results for the CGO MSL core at 1.0 T and 1.7 T are presented earlier in Fig. 13 and Fig. 14. The distributions on the SSL core surfaces

were similar. The results for the CGO SSL core at 1.0 T approximately are 40 $\mu\varepsilon$ and 50 $\mu\varepsilon$ on top and side surfaces respectively and at 1.7 T, approximately 100 $\mu\varepsilon$ and 100 $\mu\varepsilon$ on top and side surfaces. The distribution of harmonics at fixed points in the central limb (A/B/C averaged), the T-joint (D) and the corner joint (E) in the two cores are compared in Table IV. The harmonics are shown in relative form to highlight similarities and differences in the trends. Little information is lost since the levels in the SSL core were similar to those for the MSL core quantified in Table III.

The most significant findings that can be extracted from Table IV are (a) the central limb of the MSL and SSL cores experience the highest 100 Hz vibration which itself is higher in the MSL core at each flux density (b) harmonics develop in the T-joints of both cores with increasing flux density and at 1.7 T the higher harmonics develop more prominently in the SSL core (c) in the corner joint, at each flux density the 100 Hz component is higher in the SSL core but at 1.7 T the 200 Hz and 300 Hz components become significantly higher in the MSL core (d) the highest magnitudes of the higher frequency harmonics occur in the T-joints of the two cores.

It can be seen that the first two harmonics have higher amplitude because of an effect of MS and that it is a source of noise. However, such low frequency vibration is not picked up by the human ear. This is the reason why in some cases have higher vibration but have lower noise.

TABLE 4 HERE

Fig. 19 compares the harmonic spectrum of the rms velocity at points in the same three regions of the SSL and the MSL cores at 1.7 T to highlight the trends shown in Table I and IV. Considering the frequency distribution of the vibration component at 1.5 T and 1.7 T, on the limb surface the frequency component at 100 Hz of the SSL is approximately half the amplitude of the MSL configuration (approximately 0.70 mm/s on MSL core and 0.35 mm/s on SSL core), whilst there are higher amplitude of harmonic components near 1 kHz. This is the reason for higher A-weighted sound power level in the SSL core.

FIG. 19 HERE

The surface velocity in the central limb of the SSL core has a higher harmonic content than the MSL core. The overall vibration in the central limb of the SSL core is lower than of the MSL core but its impact on A-weighted noise would be higher. The trend in both corner joints is similar with very high harmonic levels, similar distribution in both core suggesting similar mechanisms, whereas in the T-joint the MSL spectrum contains relatively higher harmonic levels.

E. Comparison of single phase and three phase cores

Single and three phase cores of CGO were assembled with geometries shown in Fig. 5 using MSL joints and a clamping bolt torque of 4.0 Nm. They were magnetised at 1.5 T to 1.7 T and the A-weighted sound power level was measured. The noise output from the single phase core was around 2 dBA higher than that of the three phase core at both flux densities. The cores are identical in size and construction apart from the central limb and T-joints of the three phase core which might be expected to contribute significantly to the noise.

The out of plane rms velocity was measured with the laser vibrometer averaged over surfaces of the two cores. The average vibration of the limb of the single phase core was found to be 4 to 5 times less than that of the outer limbs of the 3 phase core although its noise output was higher. However, the joint vibration in the single phase core is considerably higher although magnetically the joints are identical. The high vibration of the T-joint would be expected to produce a noise contribution not experienced by the single phase core but in spite of this the three phase core is quieter.

It may appear surprising that the noise of the single phase core is higher and also that there does not seem to be any correlation between average surface vibration and acoustic noise. It can be partially explained by considering the time phase of the vibrations as discussed in section IV *C* but the phenomenon needs more investigation.

V. Discussion and Conclusions

The most difficult hurdle in predicting the acoustic noise of three phase transformer cores is quantifying the contribution of magnetostrictive and EM forces to the core vibration. The magnetostrictive forces can occur anywhere within the whole core volume and although the EM forces are set up in the core joints they also cause strain, hence potential vibration, throughout the whole core so it is very difficult to isolate the effect of each on localised in-plane or out of plane vibration in laminations. It is possible that they interfere with each other thus making the analysis even more complex.

The magnetostrictive forces can be minimised by use of low MS GO material hence reducing noise as illustrated in Table I but the size of the reduction depends very much on the core joint configuration, with the less common SSL configuration showing a less predictable response to low MS material.

It is impossible to accurately estimate the contribution of magnetostrictive forces to core noise just from stress sensitivity of the type shown in Fig. 1. *Incorporation of MS harmonics in the characterisation seems essential just by noting the widespread occurrence of vibration harmonics in this study which are not linked in any obvious way to the fundamental (100 Hz) component but no better means of quantifying the role of the harmonic has yet been verified*.

The type of material had no influence on noise when SSL joints were used apart from at very high flux density when the low MS HGO core unexpectedly produced highest noise. Since the EM force induced vibration should be mainly independent of the magnetic properties and flux density for a given geometry this must be due to some magnetostrictive influence not quantified in the MS curves produced in the commonly used format as shown in Fig. 1. This is most possible since it is widely accepted that harmonics of MS are a major influence on A-weighted noise and they are not accounted for in any way in these characteristics.

Rotational MS is undoubtedly larger and more anisotropic than unidirectional MS at the same peak flux density [24] so it

is often suggested as possibly being a significant source of noise in three phase cores. *However, the results shown in section IV A back up previous suggestions [32] that the degree to which it occurs in the transformer joints is much less than is widely assumed because of the high anisotropy of GO, hence it cannot be a direct cause of the high joint vibration strongly evident here.*

There is no simple relationship between the magnitude and distribution of core surface displacement or velocity and acoustic noise. MS and forces between ends of laminations in the joints cause in-plane forces expected to cause in-plane vibration throughout a core but this is said to be only relevant on SSL cores [10]. The interlaminar forces at overlap regions in joints where high normal flux is present are a source of out of plane vibration which is partly responsible for the flapping of laminations at the joints. Non-effective clamping can lead to high corner vibration but here changing the clamping pressure only caused noise changes within ±0.7 dBA which is within the limits of experimental accuracy.

The experimental results from Table I and Fig.11 show rms velocity and displacement of out of plane vibration in all the cores tested was often more than 5 times higher than in-plane values despite the fact that the origin is mainly the in-plane forces. This is related to the stiffness of the cores and needs further investigation. Previous investigation on a single phase MSL core [9] found the ratio of front to top to side vibration velocity (nm/s) to be 157:140:6 at 1.6 T. The top surface velocity could be high because there is no restraining force from the T-joints which increases the front face bending and introduces additional noise in the three phase core.

The out of plane vibration of the central limb of the three phase cores was consistently higher than that of the outer limbs. This is probably due to high strain in the T-joint where out of plan vibration is also high. The reason for the high T-joint vibration is unclear. Rotational MS might contribute to a small extent but EM forces are the more likely cause even at low flux density. Fig. 15 shows how unsymmetrical in-plane strain can cause unrestrained MS extension of perhaps 10 μm which, if constrained by the core stiffness, is sufficient to cause the central limb bending. In-plane EM forces at the joints can also cause such unsymmetrical strain.

It is significant that the noise of the single phase core is higher than that of the equivalent three phase core with the same core cross sectional area per phase and core window size although the 3 phase core is greater in volume and mass. This demonstrates the importance of the variation of the phase of the surface vibration throughout the core.

Table I shows the 200 Hz component of surface out of plane-velocity is higher than the fundamental value in the T-joint and the corner joints at 1.5 T and 1.7 T. If their A-weighted values are compared the 100 Hz component is another 10 dBA less. The harmonics in the centre limb vibration are far lower. *This infers that the corresponding high 200 Hz and 300 Hz harmonics in the noise output shown in Fig.10 are at least partly due to the corner vibrations.* Previous measurements on a full size commercial power transformer showed the dBA ratios of the 1st to 4th harmonic as approximately 1.0:0.86:0.96:0.82 [34]. The harmonic distribution in Fig. 10 is different but they both illustrate the predominance of the low frequency harmonics over the fundamental value which is commonly used as a reference. The measurements in [34] were made outside the transformer tank containing the core so the harmonic distribution could be affected by mechanical resonance, etc.

The top and side surface vibration is mainly in the plane of the laminations and probably mainly produced by a different mechanism where the 100 Hz component is dominant, possibly magnetostrictive in origin. However, the vibration harmonics on these surfaces are relatively lower than those on the front surface although the sound harmonics detected by the microphones facing these surfaces did contain higher harmonics whose distribution was somewhat similar to that of the total sound output.

Harmonics in the flux density across the butt joints might be a significant origin of vibration harmonics but we are not aware of any reports quantifying this phenomenon. MS is probably the prime cause of the vibration harmonics. However, the MS of core materials is usually characterised in terms of their fundamental (100 Hz) component as in Fig. 1.

The MS components of the strips used in this investigation up to the 10th harmonic were measured independently [23]. Under zero stress and under tension the peak to peak magnitudes were all less than 0.1 $\mu\varepsilon$ which was too close to the resolution of the measurements. At 1.7 T, 50 Hz magnetisation, under compressive stress of -10 MPa the 2nd and 3rd harmonics of the MS in the CGO were 4.3 $\mu\varepsilon$ and 3.6 $\mu\varepsilon$ respectively and the respective values for the HGO and LDR materials were 16 % and 38 % and 32 % and 70 % less respectively. This implies that the harmonic level of the MS of the LDR material is lowest but it is based on one set of conditions which might not be representative of those in an actual core.

it has been shown how bending of the front face of the three phase core can manifest itself as high vibration but this need not result in correspondingly high noise. *Harmonics of vibration and noise are not found to correlate but they dominate the frequency spectrum* so more effort is needed to find more suitable ways of characterising MS to assess its impact on the noise of particular transformer core configurations. More knowledge of the actual stress distribution within cores is needed to help characterise MS in a more knowledge based manner so the effect on lamination vibration can be estimated more reliably.

The joints are undoubtedly the major source of vibration. It is claimed here that rotational MS might not be the dominant cause but only a full analytical study of the 3-D flux distribution and the associated MS can confirm its relevance. Reliable 3-D analysis would also form a foundation for a quantitative study of core joint deformation which could lead to better understanding of the vibration mechanism needed identify was of substantially reducing core losses.

ACKNOWLEDGMENT

The investigation was carried out as part of a broader study of transformer noise. The authors are grateful for the financial support and technical input of the project sponsors; ABB AB, AK Steel Corp, Alstom Grid, Brush Transformers Ltd, GC Holdings Belgium N.V., Cogent Power Ltd, Kolektor Etra Energetski Transformatorji d.o.o., Nuova Electrofer S.p.A., Koncar Distribution and Special Transformers Inc., Legnano

Teknoelectric Company S.p.A., SGB Starksrom-Gerätebau GmbH and ThyssenKrupp Electrical Steel GmbH.

REFERENCES

[1] A. J. Moses and P. I. Anderson, "Effects of external stress on the magnetic properties of electrical steels," *Proc. of 5th Int. Conf. on Magnetism and Metallurgy (WMM'12)*. Ghent, Belgium, pp 87-100, June 2012.

[2] E. Reiplinger, "Assessment of grain-oriented transformer sheets with respect to transformer noise," *J. Magnetism and Magnetic Materials*, vol. 21 pp 257-261, 1980.

[3] Z. Valkovic, "Effect of electrical steel grade on transformer core audible noise," *J. Magnetism and Magnetic Materials*, vol. 133, pp 607-609, 1994.

[4] M. Ishida, S. Okabe and K. Sato, "Model transformer evaluation of high permeability grain-oriented electrical steels," *J. Materials Science and Technology*, vol.16, pp 223-227, 2000.

[5] M. Ishida, S. Okabe and K. Sato, "Analysis of noise emitted from three phase stacked transformer model core," *Kawasaki Steel Tech. Report*, vol.39, pp 29-35, 1998.

[6] J. Swaffield, "Causes and characterisitics of transformer noise," *JIEE*, vol.89 pp 212-224, 1942.

[7] A. Ilo, B. Weiser, T. Booth and H. Pfutzner, "Influence of geometric parameters on the magnetic properties of model transformer cores," *J. Magnetism and Magnetic Materials*, Vol. 160 pp 38-40, 1996.

[8] B. Weiser, A. Hasenzagl, T. Booth and H. Pfutzner, "Mechanisms of noise generation of model transformer cores," *J. Magnetism and Magnetic Materials*, vol. 160, pp e207-e209, 1996.

[9] B. Weiser and H. Pfutzner, "Relevance of magnetostatic forces for transformer core vibrations," *J. Phys. IV France,* vol. 08, pp Pr2-591-594, 1998.

[10] B. Weiser and H. Pfutzner, "Relevance of magnetostriction and forces for the generation of audible noise of transformer cores," *IEEE Transection on Magmetics*, vol. 36, pp 3759-3777, 2000.

[11] R. Penin, J. P. Lecointe, G. Parent, J. F. Brudny, and T. Belgrand, "Grain-Oriented Steel Rings for an Experimental Comparison of Relative Magnetostriction and Maxwell's Forces Effects," *IEEE Transactions on Industrial Electronics*, vol. 61, pp. 4374-4382, 2014.

[12] D. Snell, "Noise generated by model step lap core configuration of grain oriented electrical steel," *J. Magnetism and Magnetic Materials,* vol. 320, pp e887-e890, 2008.

[13] M. Mizokami and Y. Kurosaki, "Variation of noise and magnetostriction associated with joint types of transformer," *IEEJ Trans on Fundamentals and Materials*, vol. 134, pp 334-339, 2014. (Republished in English in *Elec. Eng. In Japan*, vol. 194, No. 2, 2016.

[14] Z. Valkovic, "Effects of transformer core design on noise level," *J. Phys. France*, vol. 08, pp Pr2-603-606, 1998.

[15] K. Jenkins and D. Snell, "Aspects of Noise associated with GO Electrical Steels in Transformer Applications," *UK Magnetics Society, Noise in Electrical Machines,* Cardiff, UK, 4th Feb 2009.

[16] J. Anger and A. Daneryd, "Noise in power transformers- Models for generation, transmission and propagation," *Magnews, UK Magnetics Society*, Spring Issue, 2009.

[17] S. L. Foster and E. Reiplinger, "Characteristics and control of transformer sound," *IEEE Transaction on Power Apparatus and Systems*, vol. PAS-100, pp 1072-1077, 1981.

[18] P. I. Anderson, A. J. Moses and H. Stanbury, "Assessment of the stress sensitivity of magnetostriction in grain-oriented silicon steel," *IEEE Transactions on Magnetics*, vol.43, pp 3467-3276, 2007.

[19] W. Gong, Z. Zhang, R. Hou, H. Wang, Z. Xu and A. Lin, "Magnetostriction and the influence of harmonics of flux density in electrical steel," *IEEE Transactions on Magnetics*, vol. 51 pp 1-4 2015.

[20] P. Hamberger, "Low noise power transformers- more energy in large cities with less noise," *Magnews, UK Magnetics Society*, Spring Issue, pp 20-23, 2009.

[21] M. Mizokami, M. Yabumoto and Y. Okazaki, Vibration analysis of a 3-phase model transformer core," *Elect. Eng. in Japan*, vol. 119, pp 1-8" 1997.

[22] P. I. Anderson, A.J. Moses, and H.J. Stanbury, "An automated system for the measurement of magnetostriction in electrical steel sheet under applied stress*." J. Magnetism and Magnetic Materials*, vol. 215, pp 714-716 2000.

[23] S. Tabrrizi, "Study of effective methods of characterisation of magnetostriction and its fundamental effect on transformer core noise," *PhD Thesis*, Cardiff University UK, December 2013.

[24] M. Enokizono, S. Kano and G. Shirakawa, "Measurement of arbitrary dynamic magnetostriction under alternating and rotational field," *IEEE Transactions on Magnetics*, Vol. 21, pp 3409-3411, 1995.

[25] T. Phophongviwat, "Investigation of the influence of magnetostriction and magnetic forces on transformer core noise and vibration," *PhD Thesis*, Cardiff University UK, August 2013.

[26] D. Snell, "Measurement of noises associated with model transformer cores," *J. Magn. Mag. Mat*., vol. 320 pp e535-538, 2008.

[27] Z. Valkovic, "Investigation of core noise levels using a dry-type transformer model," *J. Magn. Mag. Mat.*, vol.160 pp 205-6, 1996.

[28] R. G. Budynas and N. J. Keith, "*Shigley's mechanical engineering design*," 9th ed.: McGraw-Hill, New York, 2011.

[29] M. A. Jones, A. J. Moses and J. E. Thompson, "Flux distribution and power loss in the mitred overlap joint in power transformer cores," *IEEE Transactions on Magnetics*, vol. 9, pp 114-121, 1973.

[30] F. Brailsford and J. M Burgess, "Internal waveform distortion in silicon-iron laminations for magnetisation at 50 c/s," *Proc. Instn. Elect. Engrs*. vol. 108C, pp 458-XX, 1961.

[31] A. J. Moses and B. Thomas, "The spatial variation of localised power loss in two practical transformer T-joints, *IEEE Transactions on Magnetics,*" vol. MAG-9, pp 655-659, 1973.

[32] A. J. Moses, The case for characterisation of rotational losses under pure rotational field conditions," *Preglad Elekrotechniczny*, vol. 81, pp 1-4, 2005.

[33] L. Zhu, Q Yang, and R. Yan, "Numerical analysis of vibration due to magnetostriction of three phase transformer core," *Sixth International Conference on Electromagnetic Field Problems and Applications (ICEF) 2012*, pp.1,4, 19-21 June 2012.

[34] R. Girgis, J. Anger and D. Chu, "The sound of silence Design and producing silent transformers," *ABB Review*, No, 2, pp 47-51, 2008.

[35] G. Shilyashki, H. Pfützner, P. Hamberger, M. Aigner, F. Hofbauer, I. Matkovic, and A. Kenov, "The Impact of Off-Plane Flux on Losses and Magnetostriction of Transformer Core Steel," *IEEE Transactions on Magnetics*, vol. 50, pp. 1-4, 2014.

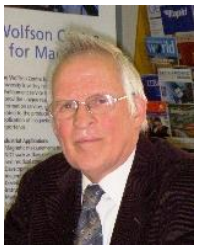

Anthony John Moses (M'87, Life Member 2015) was born in Newport, Gwent UK. He received his B.Eng. Tech. in Electrical Engineering and PhD from the University of Wales in 1966 and 1970 respectively followed by a DSc in 1990 for contribution to research into the properties and applications of soft magnetic materials.

Appointed Professor of Magnetics and Director of the Wolfson Centre for Magnetics at Cardiff University in 1992 after periods as a Lecturer, Senior Lecturer and Reader at the university. He is author of over 500 publications and supervisor of more than 100 post graduate students in themes related to the production, characterisation and applications of magnetic materials.

Professor Moses is a Fellow of the Institute of Physics and the Institution of Engineering and Technology. Past Chairman of the UK Magnetics Society and the International Organising Committee of the Soft Magnetic Materials (SMM) series of conferences. He is a member of organising and editorial committees of several international conferences and journals. Since 2012 he has been Emeritus Professor at Cardiff University where he continues his interests in properties and applications of magnetic materials.

Philip Anderson was born in Wales, UK in 1972. He received a B.Eng and MSc from Cardiff University and following this worked with Cogent Power in Newport. He received his PhD from Cardiff University in 2000 and worked at the Wolfson Centre, Cardiff University since this time as a researcher and now senior lecturer in Magnetic Engineering. His research concentrates on the production, application and characterization of soft magnetic materials. Dr Anderson is a Chartered Engineer and member of national and international standards committees on magnetic steels and alloys. He is currently a member of the international organising committees of several major conference series including Soft Magnetic Materials (SMM).

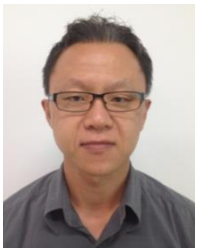

Teeraphon Phophongviwat was born in Kanchanaburi, Thailand he received his B. Eng and M. Eng in electrical engineering from the King Mongkut's Institute of Technology Ladkrabang (KMITL) in 1999 and 2002 respectively, and the PhD degree in electrical and electronic engineering from the Wolfson Centre for Magnetics at Cardiff University, UK in 2013. He is currently working at the Department of Electrical Engineering, Faculty of Engineering, KMITL, Thailand. His research interest include transformer, electrical machines, magnetic materials, finite element and optimisation techniques.

TABLE I
VARIATION OF RMS VALUES OF HARMONICS OF SURFACE VELOCITY [μm/s] AT LOCATIONS ON THE SURFACE OF THE CGO MSL CORE MAGNETISED AT 1.0 T, 1.5 T AND 1.7 T, 50 Hz.

f [Hz]	A/B/C (centre limb)			D (T-joint)			E (corners)		
	1.0 T	1.5 T	1.7 T	1.0 T	1.5 T	1.7 T	1.0 T	1.5 T	1.7 T
100	313	747	1027	351	1272	1006	348	276	957
200	11	36	153	25	849	1254	111	378	1015
300	4	10	89	32	125	682	18	334	620
400	3	19	92	10	349	294	11	96	165
500	2	17	36	2	110	442	13	142	205
600	1	7	59	3	68	271	8	92	150

TABLE II
HARMONICS OF SOUND PRESSURE [mPa] EMITTED FROM SIDE (POSITION 1) AND TOP (POSITION 9) SURFACE OF THE THREE PHASE CGO CORE MAGNETISED AT 1.0 T, 1.5 T AND 1.7 T

	Side surface			Top surface		
	1.0 T	1.5 T	1.7 T	1.0 T	1.5 T	1.7 T
100 Hz	0.65	1.1	1.5	0.4	0.55	0.5
200 Hz	0.48	2.5	5.5	0.4	0.95	0.6
300 Hz	0	0.7	4.0	0.2	0.3	0.9
400 Hz		0.3	1.6	0.11	0.2	0.3
500 Hz		0.2	0.9		0.1	0.9
500-4000 Hz	< 0.15	< 0.25	< 0.6	0.15	0.25	0.5
Total sound pressure [mPa]	34	32	36	26	23	28
Sound pressure level [dB]	65	64	65	62	61	63
A-weighted sound pressure level [dBA]	40	43	49	36	39	46

TABLE III
COMPARISON OF SOUND PARAMETERS MEASURED BY MICROPHONES ADJACENT TO FRONT, SIDE AND TOP SURFACES OF THE CGO MSL CORE

	Front		Top		Side		Average	
	1.0 T	1.7 T	1.0 T	1.7 T	1.0 T	1.7 T	1.0 T	1.7 T
Sound pressure [mPa]	29	33	26	28	34	36	29.5	34.3
Sound pressure level [dB]	63	64	62	63	65	65	63.4	64.3
A-weighted sound pressure level [dBA]	39	52	36	46	40	49	38.8	49.8

TABLE IV
COMPARISON OF HARMONIC LEVELS OF OUT OF PLANE SURFACE RMS VELOCITY [μm/s] AT POINTS IN THE MIDDLE LIMB (A/B/C), THE T-JOINT (D) AND THE CORNER JOINT (E) OF (a) MSL AND (b) SSL CGO CORES AT DIFFERENT FLUX DENSITIES.(BOLD FIGURES INDICATE HIGH VALUES COMPARED TO THE OTHER CONFIGURATION)

(a) MSL,(1.0-1.7 T, 100-600 Hz harmonics)

f [Hz]	A/B/C (Centre limb)			D (T-joint)			E (Corners)		
	1.0 T	1.5 T	1.7 T	1.0 T	1.5 T	1.7 T	1.0 T	1.5 T	1.7 T
100	**313**	**747**	**1027**	**351**	1272	**1006**	348	276	957
200	11	36	**153**	25	**849**	1254	111	**378**	**1015**
300	4	10	**89**	32	**125**	682	18	334	**620**
400	3	19	**92**	10	349	294	11	96	165
500	2	17	**36**	2	110	**442**	13	142	205
600	1	7	59	3	68	**271**	8	**92**	**150**
Total (RMS)	**223**	**544**	**749**	187	492	673	**237**	**393**	**595**

(b) SSL (1.0-1.7 T, 100-600 Hz harmonics)

f [Hz]	A/B/C (Centre limb)			D (T-joint)			E (Corners)		
	1.0 T	1.5 T	1.7 T	1.0 T	1.5 T	1.7 T	1.0 T	1.5 T	1.7 T
100	91	359	488	301	1258	464	**755**	**1301**	**1169**
200	13	**58**	89	**150**	690	**1475**	**283**	268	195
300	3	**23**	38	31	35	**890**	**54**	**353**	378
400	2	23	74	**22**	333	517	**18**	**134**	**328**
500	3	23	21	**24**	**170**	370	8	43	22
600	9	**35**	**153**	**16**	**114**	245	5	59	135
Total (RMS)	115	277	420	**213**	**809**	**1146**	106	326	479

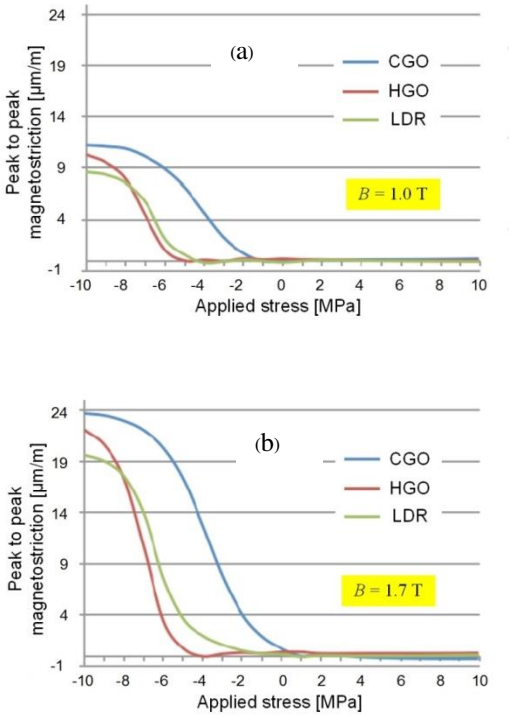

Fig. 1. Stress sensitivity of the peak to peak MS of strips of CGO, HGO and LDR magnetised along their RDs at 50 Hz (a) 1.0 T peak magnetisation, (b) 1.7 T peak magnetisation.

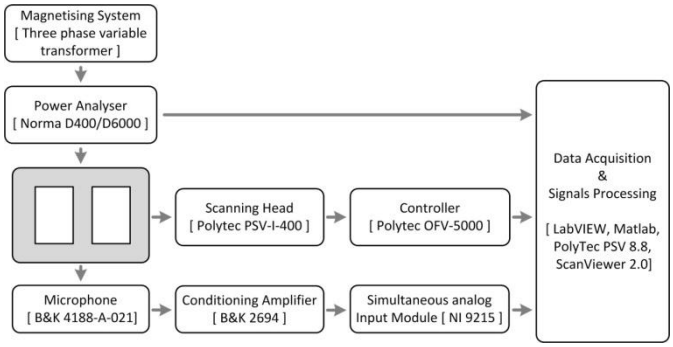

Fig. 2. Overview of the transformer core magnetising method and the noise and vibration measurement process.

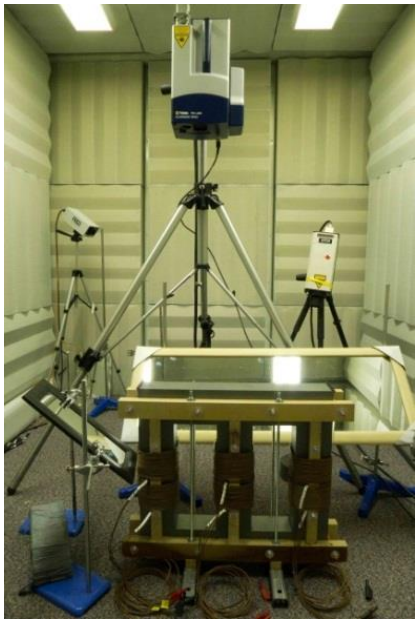

Fig. 3. Transformer core and vibrometer set up in the hemi-anechoic chamber.

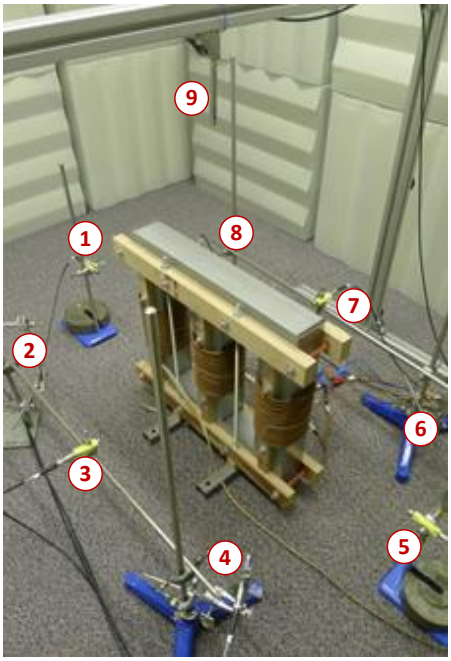

Fig. 4. Locations of microphones around and above a core under test in the acoustic chamber.

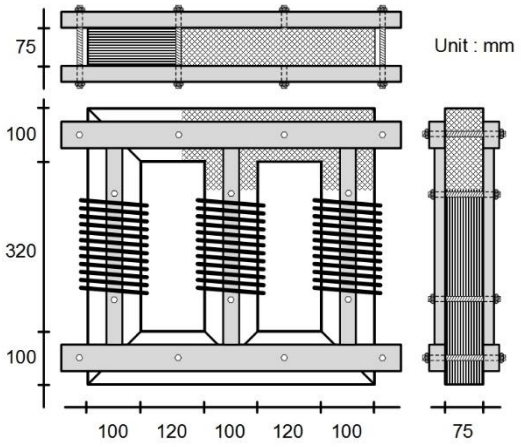

a) Three phase core

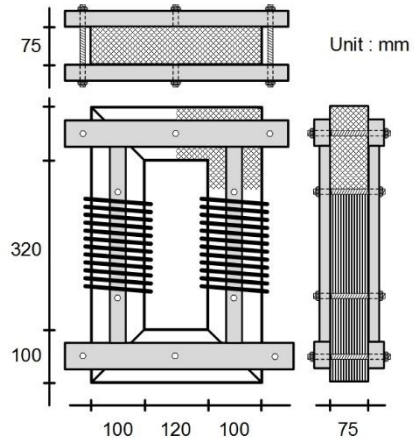

b) Single phase core

Fig. 5. Front views showing winding and clamping arrangement (a) a three phase core, 115 kg. (b) a single phase core, 72 kg.

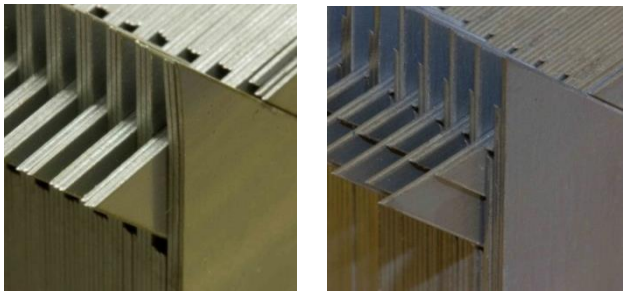

a) b)

Fig. 6. Examples of corner joints (a) single step with 3 laminations per layer and 6 mm of length overlap shift (b) a 4 step MSL joint with one laminations per layer and 6 mm overlap length (these are not the values used in the investigation but are included for illustration).

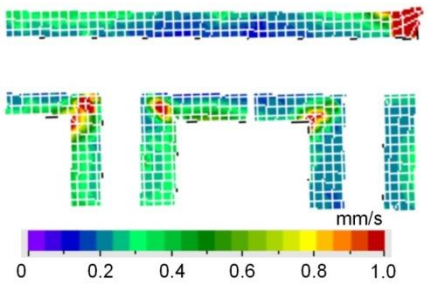

a) 2.0 N-m

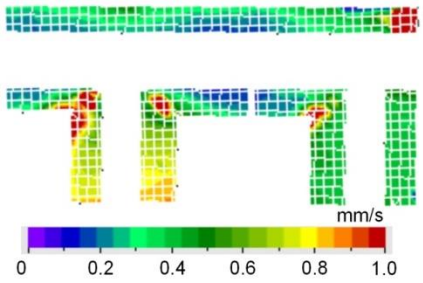

b) 4.0 N-m

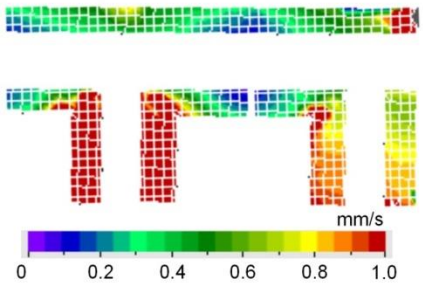

c) 6.0 N-m

Fig. 7. Distribution of rms component of out of plane vibration measured on a CGO MSL core at 1.7 T with clamping torques of (a) 2 Nm (b) 4 Nm (c) 6 Nm.

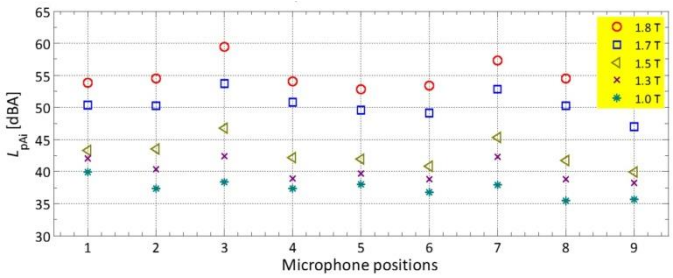

Fig. 8. Variation of averaged (3 trials) A-weighted sound pressure level from microphone placed on the prescribed contour (positions 1 to 8) and above (position 9) of three phase MSL CGO core at flux densities of 1.0 T to 1.8 T, 50 Hz.

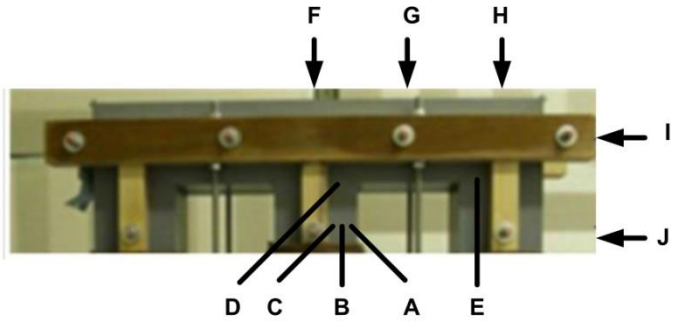

Fig. 9. Positions at which localised vibration was measured on the surface of the three-phase, MSL CGO core

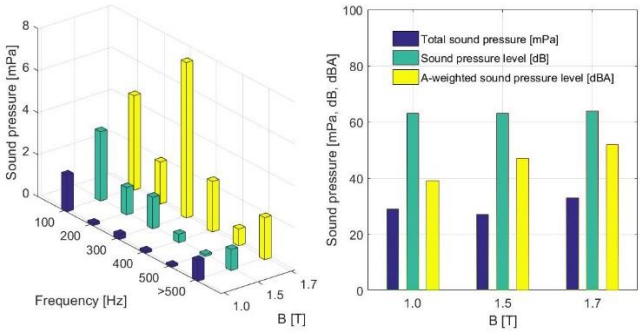

Fig. 10. Harmonics of sound pressure [mPa] emitted from front surface of the three phase CGO core at 1.0 T, 1.5 T and 1.7 T, 50 Hz (detected by microphone 3)

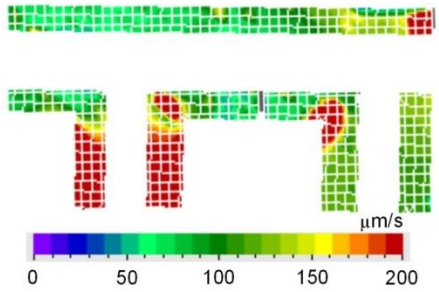

a) 1.0 T

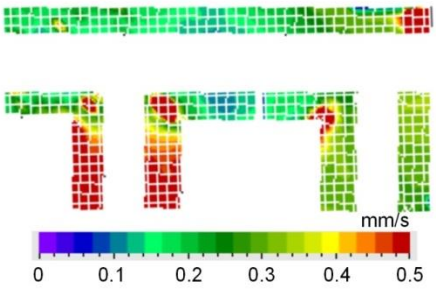

b) 1.5 T

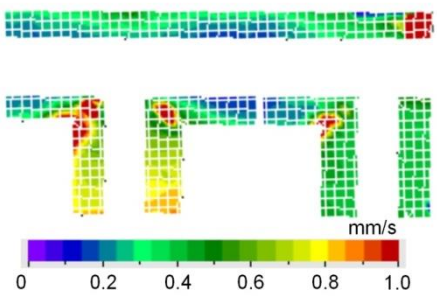

c) 1.7 T

Fig. 11. RMS vibration velocity distribution on the front surface of the CGO MSL core at (a) 1.0 T (b) 1.5 T (c) 1.7 T.

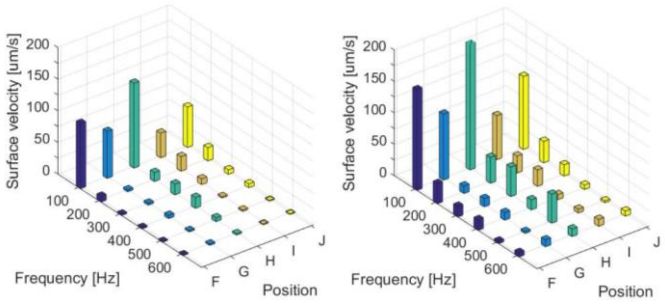

Fig. 12. Variation of RMS values of harmonics of surface velocity [μm/s] at locations on the front and side surfaces of the CGO MSL three-phase core magnetized at 1.0 T to 1.7 T, 50 Hz.

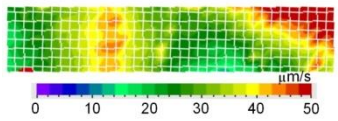

a) 1.0 T

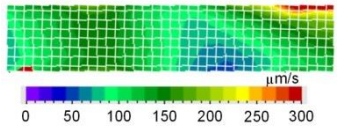

b) 1.7 T

Fig. 13. Distribution of in-plane component of rms velocity (μm/s) on the top surface of the CGO, MSL core at (a) 1.0 T, (b) 1.7 T.

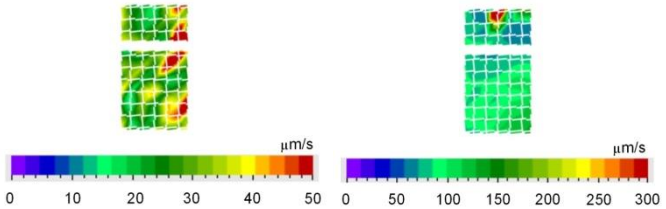

a) 1.0 T b) 1.7 T

Fig. 14. Distribution of in- plane component of rms velocity (μm/s) on the side surface of the CGO, MSL core at (a) 1.0 T, (b) 1.7 T.

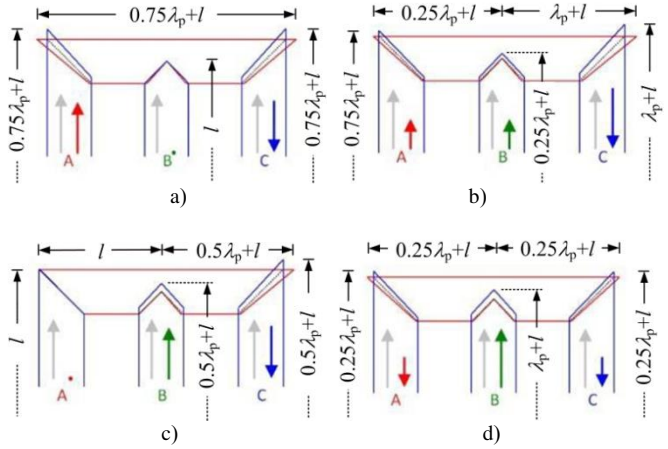

a) b)

c) d)

Fig. 15. Representations of magnitude and direction of instantaneous flux density and simulated magnetostrictive distortion at (a) ωt=0° and 180° (b) ωt=30° (c) ωt=60° (d) ωt=90°

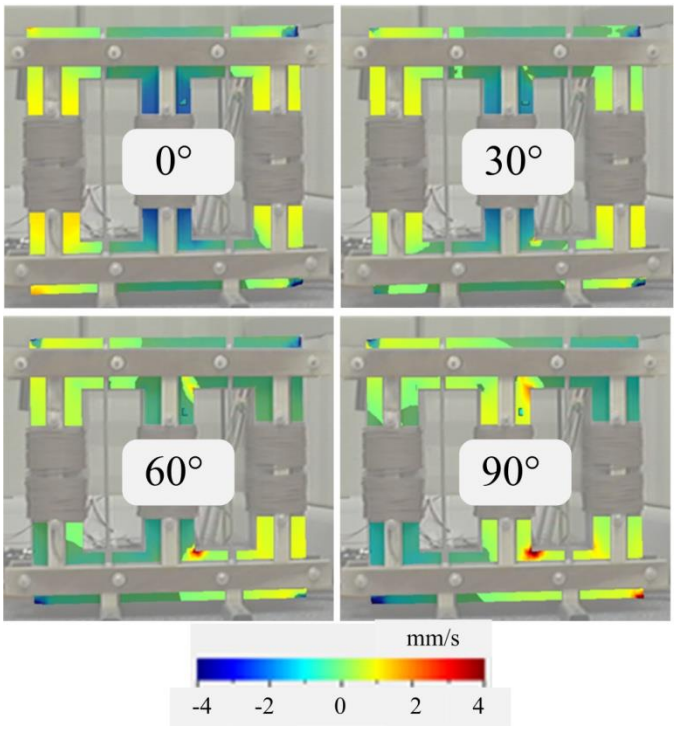

Fig. 16. Measured instantaneous velocity contour on the front surface of the CGO MSL core with clamping pressure of 0.33 MPa at ωt = 0°, (180°) , 30°, 60°, 90° at B_p=1.7 T.

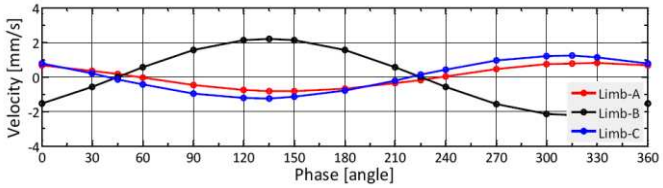

Fig. 17. Comparison of measured variation of instantaneous fundamental velocity (100 Hz) at the centre and half height on each limb during one cycle of magnetisation between centre limb (Limb-B) and outer limbs (Limb-A and Limb-C) at 1.5 T, 50 Hz.

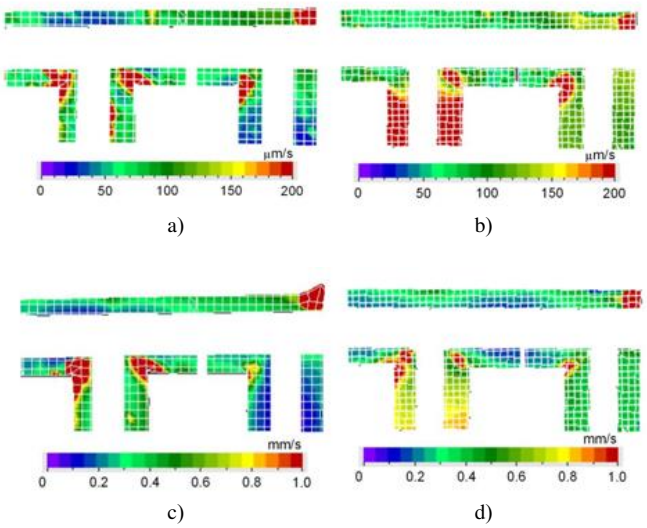

Fig. 18. Distribution of rms value of localised out of plane velocity of the front surface of CGO cores (a) SSL, 1.0 T, (b) MSL, 1.0 T (c) SST, 1.7 T (d) MSL, 1.7 T.

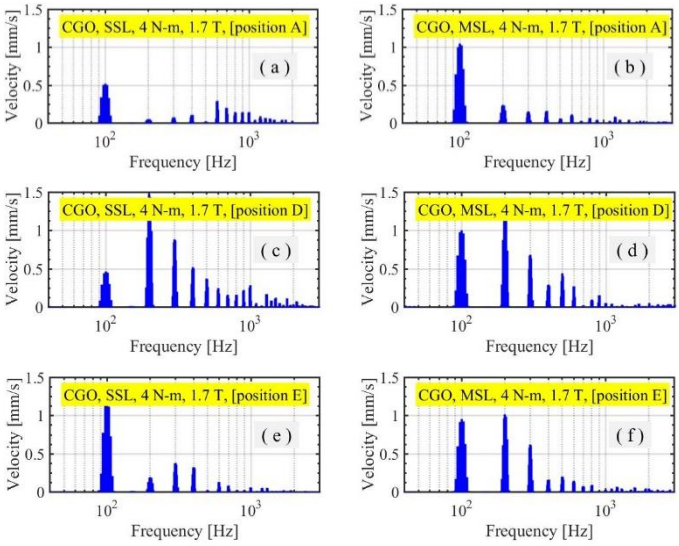

Fig. 19. Frequency distribution of out of plane rms harmonic components of vibration velocity. 1.7 T, 4.0 Nm bolt torque (a) central limb, position A on SSL core (b) central limb, position A on MSL core (c) corner joint region, position D on SSL core (d) corner joint region, position D on MSL core (e) T-joint region, position E on SSL core (f) T-joint region, position E on SSL core.